Detuning, Resonances and the Complete Non–linear Model determined from Turn–by–Turn Pick–up Data

F. Schmidt, CERN, Geneva, Switzerland

Abstract

Recently, it has been demonstrated that a sufficiently precise FFT spectrum can be used to construct a complete non–linear model of an accelerator like the LHC. Each spectrum line in the FFT from turn–by–turn tracking data has one corresponding term in the distortion function in resonance basis. This distortion function is normally derived from a one–turn map using Normal–Form techniques. Using the same tools one can perform the inverse operation from the distortion function back to the one–turn map which represents the non–linear model of the accelerator. The method requires small amplitude oscillation and is applied in a order by order fashion starting with the sextupole terms.

This method should work equally well for experimental data from turn–by–turn pick–ups given that the noise level of the measurement system is low enough. An additional advantage is the fact, that all linear parameters can be measured as well such that a complete description of the linear and non–linear model should be obtainable.

1 INTRODUCTION

Since many years perturbation theory [1] and more recently the Normal Form [2–5] techniques have been used to understand nonlinear motion of single particles in hadron accelerators. This has proven to be very useful in the design phase of an accelerator. When it comes to existing machines these sophisticated tools have been rarely in use up to now. In part this is due to the complexity of the theory but also due to the fact that a nonlinear model of the accelerator cannot be predicted easily. Checking such a model experimentally [6, 7] may prove even more difficult.

One well documented attempt to overcome this problem has been made by Bengtsson [8]. In the framework of the first order perturbation theory he has studied how the real spectra from tracking or experimental turn-by-turn data can be related to resonances. This study has stopped short of a complete solution. An important prerequisite to his analysis was a tune measurement technique superior to the standard FFT [9]. Similar attempts were performed in the field of celestial mechanics [10].

Recently, new techniques were developed [11, 12], allowing an even more precise determination of the tunes. It seems therefore appropriate to review the link between experimental data and theoretical models. The frequency map analysis by Laskar [11] can be used not only to derive the tune, but also to find spectral lines in descending order of magnitude. It has already been shown how these spectra can be applied to remove from a sequence of tracking data unwanted regular complexity. Moreover, this method has been successfully used to correct resonances excited by sextupoles [13].

2 SOME THEORY

The theory has been developed in depth in Ref. [14] a short outline of which can be found in this section.

Complex Fourier spectrum of normalised coordinates can be written as:

$$\hat{x}(N) - i\hat{p}_x(N) = \sum_{j=1}^{\infty} a_j e^{i[2\pi(m_j\nu_x + n_j\nu_y)N + \psi_j]} \qquad m_j, n_j \in \mathbf{Z}, \tag{1}$$

The connection between one–turn maps and Normal Form can be conveniently described using the Map – Normal Form Diagram (for details see [3, 5]):

$$\begin{array}{ccc} \mathbf{x} & \xrightarrow{\quad\mathbf{M}\quad} & \mathbf{x}' \\ {\scriptstyle\mathbf{\Phi}^{-1}}\downarrow & & \downarrow{\scriptstyle\mathbf{\Phi}^{-1}} \\ \zeta & \xrightarrow[\quad\mathbf{U}\quad]{} & \zeta' \end{array} \tag{2}$$

Generating function F and Hamiltonian H are given by:

$$\mathbf{\Phi} = e^{:F(J,\phi):} \quad , \quad \mathbf{U} = e^{:H(J):} \quad . \tag{3}$$

The Normal Form coordinates can then be written as:

$$\zeta = e^{-:F_r:}\mathbf{h}, \quad h_z^{\pm} = \hat{z} \pm i\hat{p}_z, \tag{4}$$

with the generating function in resonance basis:

$$F_r = \sum_{jklm} f_{jklm} {\zeta_x^+}^j {\zeta_x^-}^k {\zeta_y^+}^l {\zeta_y^-}^m \tag{5}$$

or

$$F_r = \sum_{jklm} f_{jklm} (2I_x)^{\frac{j+k}{2}} (2I_y)^{\frac{l+m}{2}} \times e^{-i[(j-k)(\psi_x+\psi_{x_0})+(l-m)(\psi_y+\psi_{y_0})]}. \tag{6}$$

The generating function in action leads to:

$$\mathbf{h} = e^{:F_r:}\zeta = \zeta + [F_r, \zeta] + \frac{1}{2}[F_r, [F_r, \zeta]] + \cdots \tag{7}$$

The evolution of linearly normalised coordinates can be written as:

$$\begin{aligned} h_x^-(N) \quad &= \quad \sqrt{2I_x} e^{i(2\pi\nu_x N + \psi_{x_0})} \\ &-2i \sum_{jklm} j f_{jklm} (2I_x)^{\frac{j+k-1}{2}} (2I_y)^{\frac{l+m}{2}} \times \\ &e^{i[(1-j+k)(2\pi\nu_x N + \psi_{x_0}) + (m-l)(2\pi\nu_y N + \psi_{y_0})]}. \end{aligned} \tag{8}$$

As a consequence the terms of the generating function and the spectral lines are related as follows:

	Generating Function	Spectral Line
Amplitude	$\lvert f_{jklm}\rvert$	$\lvert HSL_{jklm}\rvert = 2\cdot j\cdot (2I_x)^{\frac{j+k-1}{2}}(2I_y)^{\frac{l+m}{2}}\lvert f_{jklm}\rvert$ $\lvert VSL_{jklm}\rvert = 2\cdot l\cdot (2I_x)^{\frac{j+k}{2}}(2I_y)^{\frac{l+m-1}{2}}\lvert f_{jklm}\rvert$
Phase	ϕ_{jklm}	$PHSL_{jklm} = \phi_{jklm} + (1-j+k)\psi_{x_0} - (l-m)\psi_{y_0} - \frac{\pi}{2}$ $PVSL_{jklm} = \phi_{jklm} - (j-k)\psi_{x_0} + (1-l+m)\psi_{y_0} - \frac{\pi}{2}$

3 APPLICATION IN TRACKING STUDIES

3.1 Fourth Order Resonance

In this section the method is applied to the well studied LHC lattice version 4 [15]. A set of 60 realizations of the random multipolar errors, called seeds in the following, are included in the dipoles and quadrupoles. For each seed a set is generated of 10^4 tracking data starting with a small initial amplitude of $1\ \sigma$. In this region of phase space the amplitude dependence of the lines is to a very good approximation quadratic for the lines generated by third order terms and cubic for the lines generated by fourth order terms. Therefore, it can be concluded that higher order contributions are not relevant at $1\ \sigma$. Those quadratic sextupoles contributions to the octupole resonances can be neglected, knowing that the sextupole contributions, which are largest in the main dipoles, are quasi–locally corrected. In parallel, the maps and the resonant Hamiltonian in resonance basis are calculated using the DaLie program [16]. As an example, Fig. 1 shows that the Hamiltonian terms of the regular resonance $(2,-2)$ can be predicted with excellent precision from the line spectra of all 60 seeds.

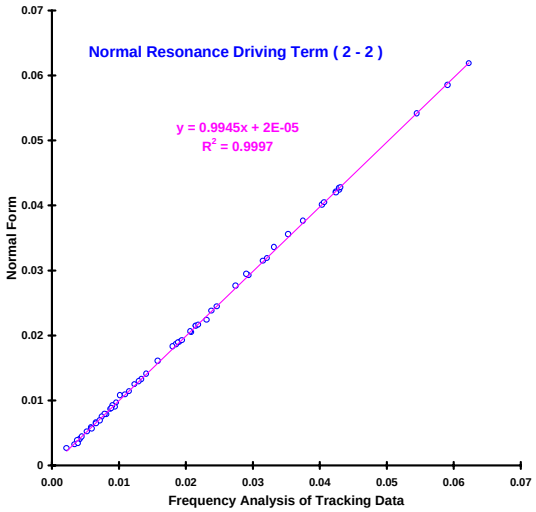

Figure 1: Hamiltonian Term from Normal Form and from Tracking Data for 60 Seeds of the LHC Lattice Version 4

3.2 Reduction of Phase Space Deformations

In a first example (LHC case in Fig. 2a, c) the do-nut shaped horizontal phase space is reduced to a near perfect circle by removing the first 100 dominant lines. It goes without saying that the tune line has to be kept. This procedure does not introduce high order distortions which tend to spoil the usefulness of perturbative techniques like Normal Form.

The strong reduction of phase space distortion can be applied to sharpen the method for detecting the onset of chaos [17]. In Fig. 2b a typical case is shown of the evolution of the angular distance in phase space of initially close–by particles. In the case of regular motion a linear increase of this distance is expected. The large variations of the distance may make it difficult however to decide about the nature of the particle motion.

The subtraction of lines (compare part d.) to part b.)) offers an easy and reliable method to reduce these variations.

The most difficult test is the study of motion close to resonance structures. The large five islands (SPS case in Fig. 2a) can indeed be reduced to points by the subtraction of lines as seen in part b.). The one essential precondition of this method is however the existence of a well defined tune. The method therefore fails in the case of chaotic motion, here achieved by approaching the vicinity of the separatrix motion. The subtraction of 100 lines that transform part c.) into part d.) does no longer simplify the complexity in phase space.

3.3 The Correction of the Resonances in the LHC

A possible exploitation of the techniques discussed so far consist in the correction of the resonance contributions generated by the nonlinear elements in an accelerator lattice. For this purpose tracking data of a realistic LHC model are analysed.

Following well established strategies for the correction of the resonances [18] one has to to identify the location and the strength of a set of correctors families to compensate the third order resonances $(3,0)$ and $(1,2)$. A family of sextupolar spool pieces, normally used to correct the average b_3 component along the lattice was split into several families to compensate the cosine and sine term of the two resonance. Using tracking data at each location of the correctors the best places for correctors could be identified, i.e. longitudinal locations where the oscillations of the lines have their extreme values (Fig. 3). Two resonances were corrected simultaneously each with two correction family while keeping the b_3 corrected on average. In this way the amplitude of the lines could be reduced by more that 50%. The resulting reduction of the phase space distortions is clearly visible in Fig. (4). In the tracking (Tab. 3.3) it can be seen that the double resonance correction leads to an improvement of the dynamic aperture of almost 10%.

Table 1: Improvement of Dynamic Aperture due to Resonance Correction

Stability Border	Uncorrected LHC lattice	Correction of (3,0) & (1,2) Resonance
Regular Motion	15.5	16.9
Strong Chaos	16.0	17.1
Lost before 1000 Turns	16.9	18.0

4 EXPERIMENTS AT ACCELERATORS

4.1 List of Observables

This FFT based method should allow to measure all linear and nonlinear observables relevant to single particle dynamics. In particular the aim is to measure the following properties:

- Phase advance between pickups
- β–beating
- Linear coupling
- Chromaticity
- Detuning versus amplitude
- Driving terms of resonances
- Full non–linear model of the accelerator

It goes without saying that a pick–up system of high quality is available around the ring. In the future it remains to be shown that the methods is applicable in the presence of pick–up noise and the unavoidable decoherence of the pick–up signal due to filamentation. The following experimental results are first recorded in Ref. [19].

4.2 SPS experiment

The SPS is an ideal test bed for this kind of investigation. The machine has practically no multipolar components so that particles exhibit mainly linear oscillations. Moreover, closed orbit, linear coupling and chromaticity have been well corrected. This "ideal" machine is made non–linear with the use of eight strong sextupoles.

In the experiment, the beam is kicked to various amplitudes and the turn–by–turn data is recorded by all pickups in one sixth of the machine (to which the SPS turn–by turn recording system is presently limited).

As expected from earlier experiments [20] the detuning as a function of the linear invariant (Fig. 6a) is very well predicted by tracking (all solid lines in Fig. 6 are tracking results obtained with SixTrack [21]). Very promising is the agreement between the tracking and the experiment for the (3,0) resonance (Fig. 6b), the experimental data are systematically lower by a few percent only. When studying the first (1,0) resonance (Fig. 6c) a problem of the closed orbit measuring system becomes apparent. This line is the amplitude dependent offset of the FFT signal after the kick. To calculate this line one has to measure and subtract the signal offset before the kick which was not possible with sufficient precision. Moreover, the number of data samples were limited to 170 turns and there had been unavoidable electronic spikes. Lastly, the other (1,0) resonance (Fig. 6d)) is presented which should suffer less from the limitations of the measurement system. Indeed, there is less noise signals in that case. However, there is a significant discrepancy with the tracking data which remains to be understood.

4.3 LEP experiment

The electron storage ring LEP was used for another experiment. Five different cases were studied with the 90/60 optics used for physics runs in 1997: one tune close to the (3,0) resonance and two tunes at increasing distance to that resonance. In the latter two cases the beam was kicked to 2 different amplitudes (each case is represented by another symbol in Fig. 7). In Fig. 7a the detuning curves are recorded with a sliding window in tune for two different kick strengths. Both curves lie fairly well on top of each other. The effect of radiation can be directly observed and there is no sign of filamentation [22]. Moreover, the detuning is well predicted by tracking (solid line as calculated with MAD [23]). Both terms of the (1,0) resonance (part c.) and d.) of Fig. 7) show good agreement

between the tracking and the experiment after inclusion of radiation (the straight curve in part c.) is obtained without radiation). However, the (3,0) resonance has a significant discrepancy with the tracking data even when radiation is properly treated. There is almost a factor 10 between experiment and tracking. Although there is not yet a full understanding of the cause of this difference it can probably be addressed to random sextupole components which are not included in the tracking.

5 CONCLUSIONS

It has been shown that the tune line spectrum can serve as a powerful tool to deal with strong nonlinearities in single particle motion. It is appealing for accelerator designer to have a tool that works without involved mathematical apparatus. It works very well in simulations and is expected to be equally useful in machine experiments. In fact, it has been demonstrated that these lines can be used to suppress unwanted phase space distortions and to correct resonances in a non-perturbative manner.

Preliminary experiments show a promising similarity between experiment and theory. In upcoming experiments it will be studied to which extent this technique allows the evaluation of nonlinearities and their correction.

6 REFERENCES

[1] A. Schoch, "Theory of linear and non–linear perturbations of betatron oscillations in alternating gradient synchrotrons", CERN 57–21, (1958).

[2] A. Bazzani et al., "Normal forms for Hamiltonian maps and nonlinear effects in a particle accelerator", Nuovo Cim., B **102**, pp. 51–80 (1988).

[3] M. Berz, É. Forest and J. Irwin, "Normal form methods for complicated periodic systems: a complete solution using differential algebra and lie operators", Part. Acc. **24**, pp. 91–107 (1989).

[4] M. Berz, "Differential-algebraic description of beam dynamics to very high orders", Part. Acc. **24**, pp. 109–124 (1989).

[5] A. Bazzani, E. Todesco, G. Turchetti and G. Servizi, "A normal form approach to the theory of nonlinear betatronic motion", CERN 94–02, (1994).

[6] W. Fischer, M. Giovannozzi and F. Schmidt, "The dynamic aperture experiment at the CERN SPS", CERN SL/95–96 (AP), Physical Review E Vol. **55**, Number 3, p. 3507, March 1997.

[7] O. Brüning, W. Fischer, F. Schmidt and F. Willeke, "Comparison of measured and computed dynamic aperture for the SPS and the HERA proton ring", presented at the "LHC95 International Workshop on Single–particle Effects in Large Hadron Colliders", Montreux, October 1995.

[8] J. Bengtsson, "Non-Linear transverse dynamics for storage rings with applications to the low-energy antiproton ring (LEAR) at CERN", CERN 88–05, (1988).

[9] E. Asseo, J. Bengtsson and M. Chanel, "Absolute and high precision measurements of particle beam parameters at CERN antiproton storage ring LEAR using spectral analysis with correction algorithms", Fourth European Signal Processing Conference, edited by J. L. Lacoume et al., North Holland, Amsterdam, pp. 1317–1320 (1988).

[10] J. Laskar, "Secular evolution of the solar system over 10 million years", Astron. Astrophys. **198**, pp. 341–362 (1988).

[11] J. Laskar, C. Froeschlé and A. Celletti, "The measure of chaos by the numerical analysis of the fundamental frequencies. Application to the standard mapping", Physica D **56**, pp. 253–269 (1992).

[12] R. Bartolini, A. Bazzani, M. Giovannozzi, W. Scandale, and E. Todesco, "Tune evaluation in simulations and experiments", Part. Acc. **56**, pp. 167–199 (1996).

[13] R. Bartolini and F. Schmidt, "Evaluation of non-linear phase space distortions via frequency analysis", LHC Project Report 98 and in the proceedings of the workshop on: "Nonlinear and Collective Phenomena in Beam Physics", Arcidosso, September 1996.

[14] R. Bartolini and F. Schmidt, "Normal Form via Tracking or Beam Data", LHC Project Note 132 (revised December 1999), Part. Accel. **59**, pp. 93–106, (1998), http://wwwslap.cern.ch/frs/report/lines97.ps.gz.

[15] M. Böge and F. Schmidt, "Tracking studies for the LHC optics version 4 at injection energy", LHC Project Report 103, presented in part at the Particle Accelerator Conference, Vancouver, May 1997.

[16] É. Forest, "The DaLie code", 1986, unpublished.

[17] F. Schmidt, F. Willeke and F. Zimmermann, "Comparison of methods to determine long–term stability in proton storage rings", Part. Accel. **35**, 1991, pp. 249–256.

[18] G. Guignard, "A General Treatment of Resonance in accelerators", CERN 76–12, 1976.

[19] R. Bartolini, L.H.A. Leunissen, Y. Papaphilippou, F. Schmidt, A. Verdier, "Measurement of Resonance Driving Terms from Turn–by–Turn Data", 1999 Particle Accelerator Conference - PAC '99 New York City, NY, USA , CERN-SL-99-032 AP, http://wwwslap.cern.ch/frs/report/TUP36.ps.gz.

[20] W. Fischer et al. , Phys. Rev. E Vol. **55**, no. 3, 3507 (1995).

[21] F. Schmidt, CERN SL 94–56 (AP).

[22] A.–S. Müller, 7^{th} LEP Perf. Workshop, CERN SL 97–06 (DI).

[23] H. Grote and C.H. Iselin, CERN SL 90–13 (AP).

a.)

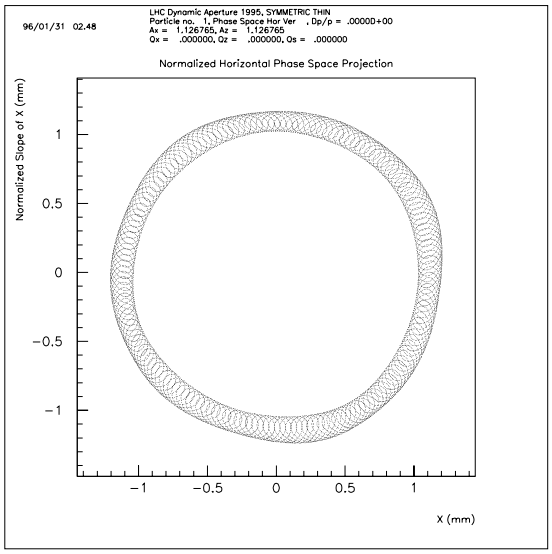

b.)

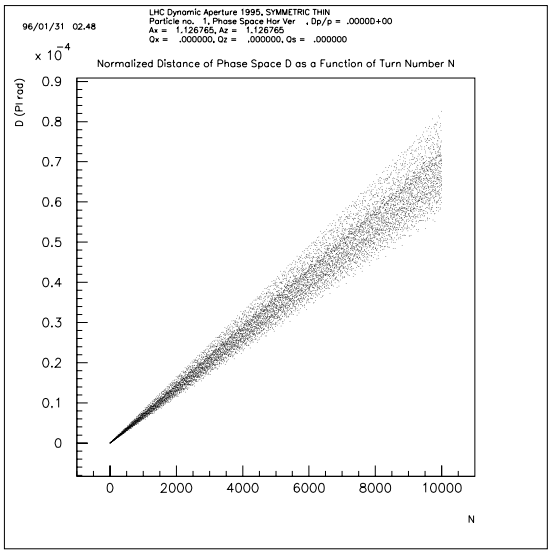

c.)

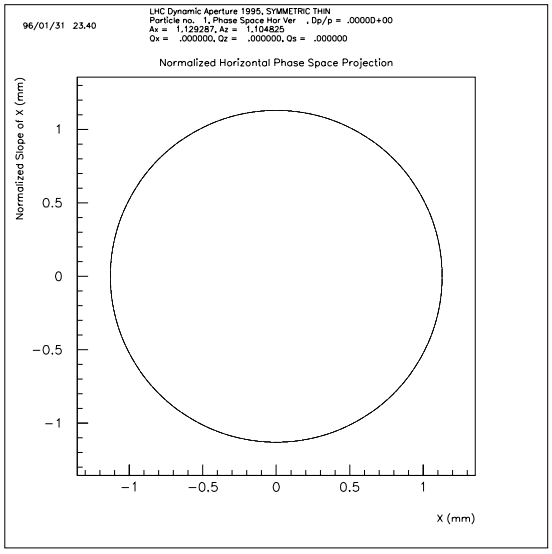

d.)

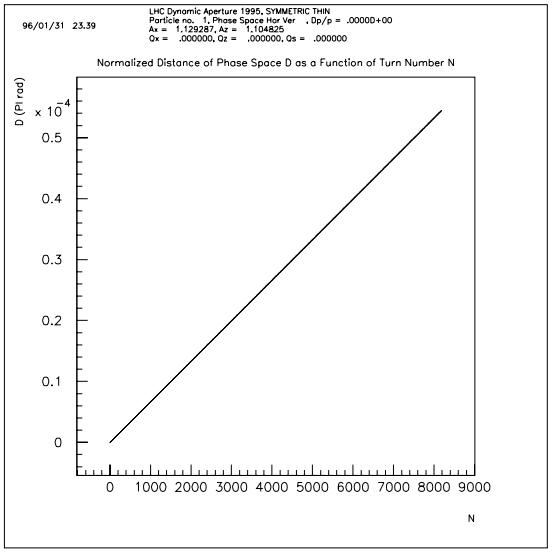

Figure2: Reducing Phase Space Distortions by Subtraction of dominant Lines
Part a.) shows a typical horizontal phase space plot of nonlinear particle motion in a LHC structure. The linear increase of the distance of two initially close-by particles indicates that the motion is regular, that is to say stable forever. Taking out the most dominant lines (with the exception of the tune line) reduces the phase space to a near perfect circle part c.). Moreover the increase of the distance in phase space, the distance in phase space, which is shaped like a wedge as seen in part b.), reduces to a thin line after the subtraction part d.).

a.)

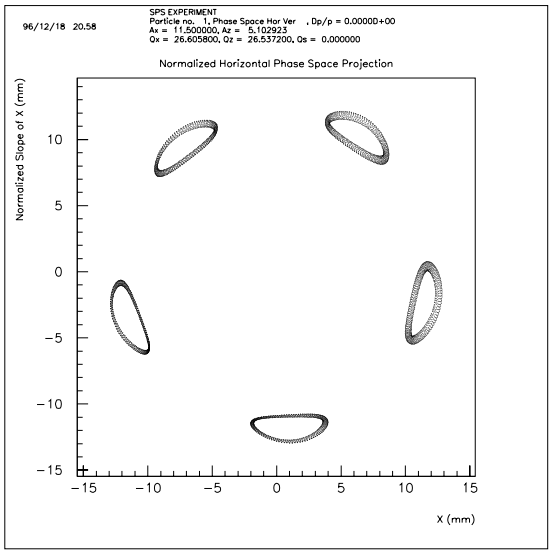

b.)

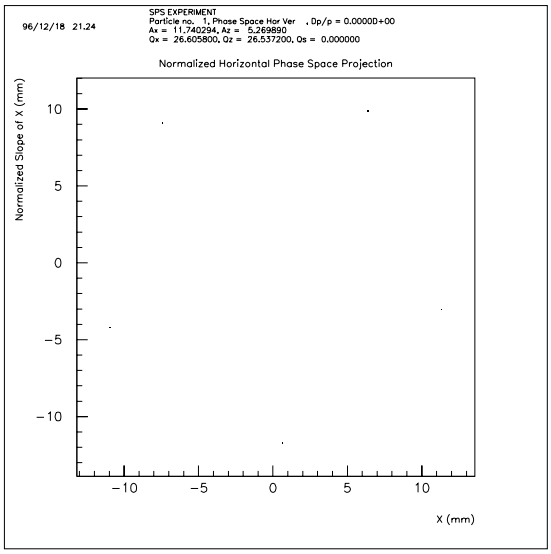

c.)

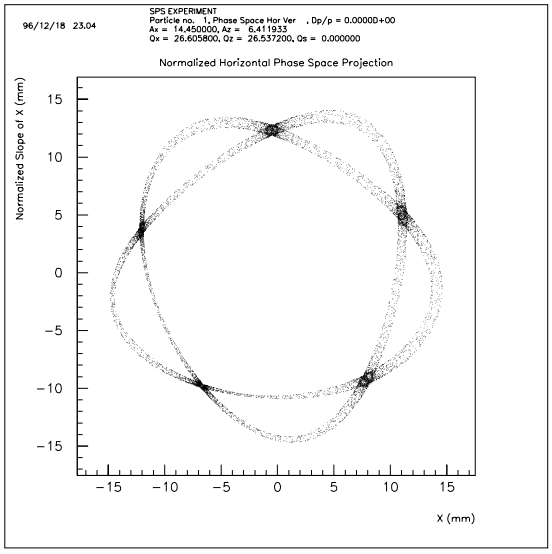

d.)

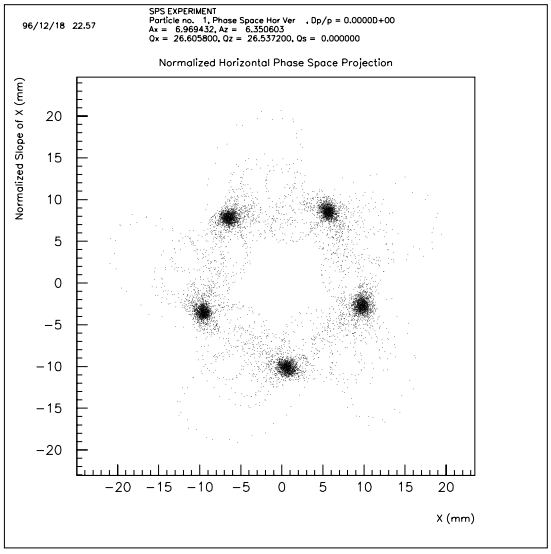

Figure 3: Reducing Phase Space Distortions close to 5^{th} Order Resonance
The motion close to a 5^{th} order resonance is shown in part a.). Taking out the 100 largest lines while keeping the tune line reduces the islands to points which are just visible in part b.). The method works of course only for regular motion. Once chaotic motion is considered, here by approaching the separatrix part c.), the subtraction of lines no longer leads to point-like objects part d.). On the contrary, one can argue that the phase space has become more distorted after this subtraction.

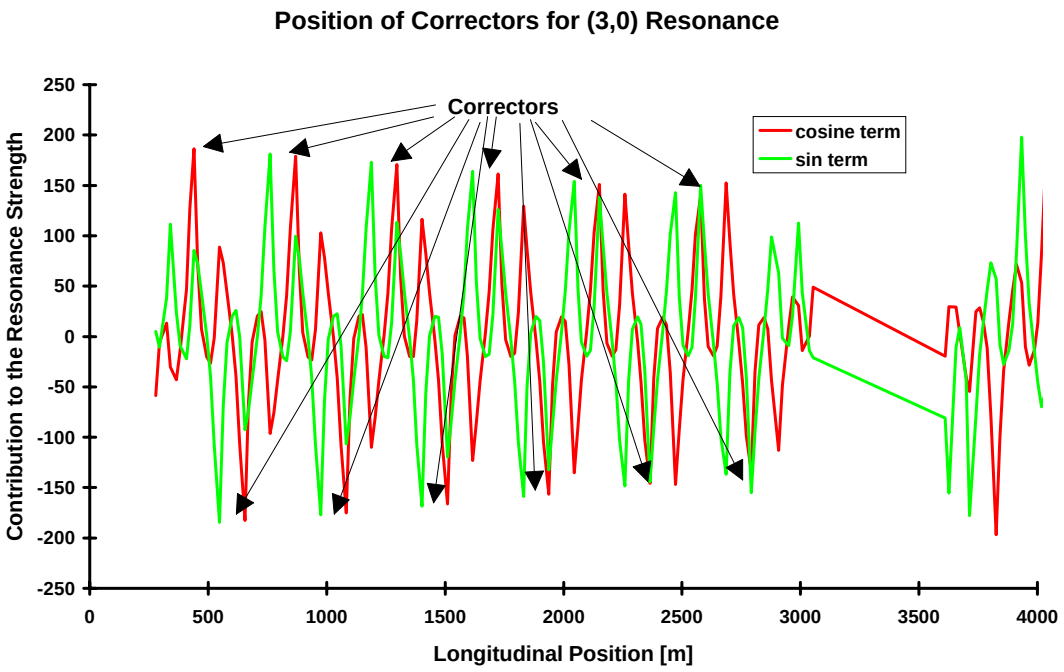

Figure 4: Choosing best places for correcting the (3,0) resonances with sextupoles

a.) b.)

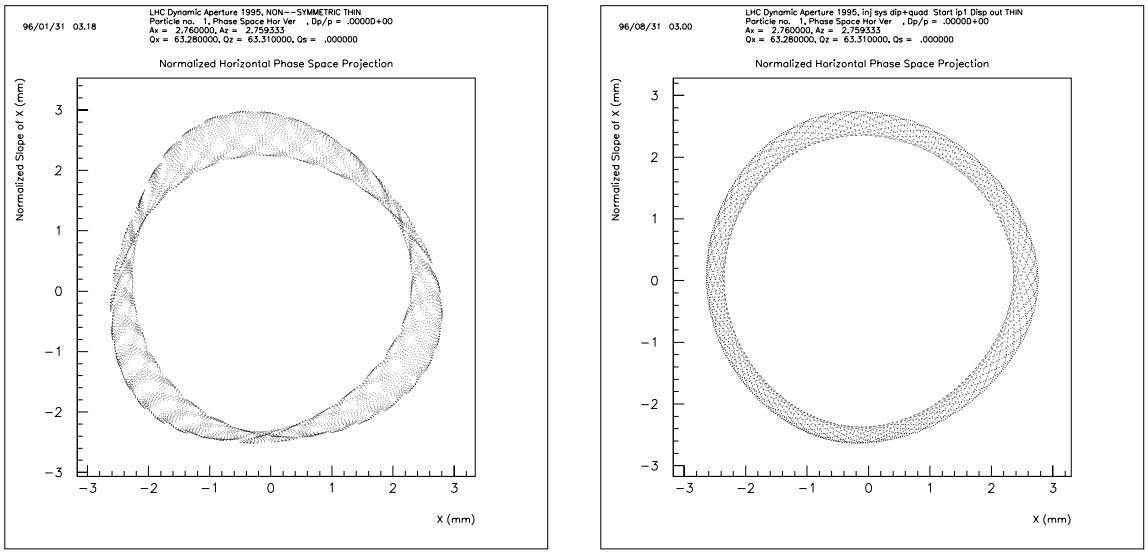

Figure 5: Reduction of Phase Space Distortion due to Correction of Resonances
In part a.) the horizontal phase space of particle motion is shown in a LHC lattice with the (3,0) and the (1,2) resonance strongly excited. These resonances have been corrected resulting in the corresponding phase space projection as depicted in part b.).

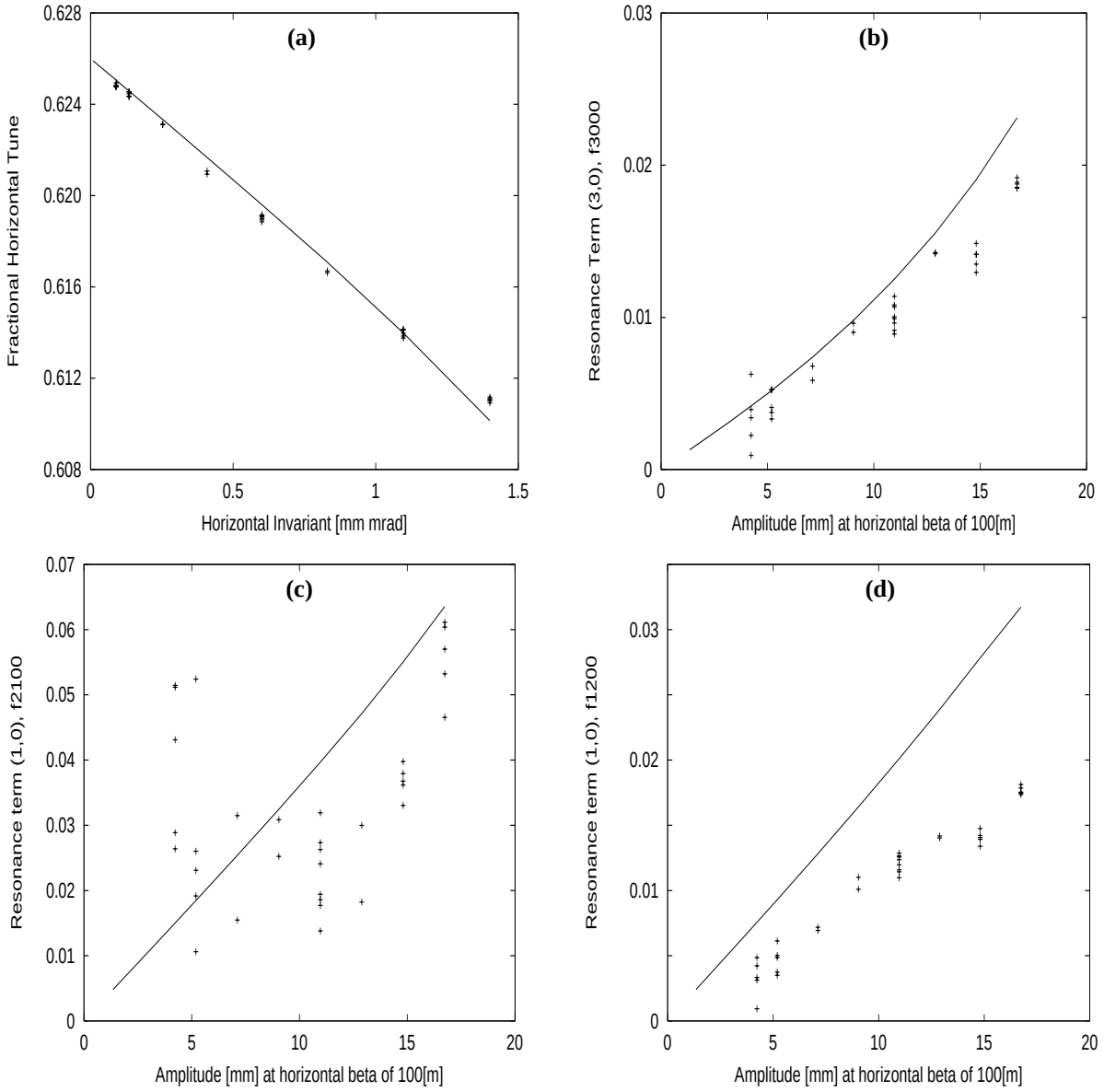

Figure 6: Detuning and First Order Sextupole Driving Terms
Part (a): Detuning versus linear Invariant I_x; Part (b): (3, 0) Resonance versus Amplitude;
Part (c): (1, 0) Resonance (f_{2100}) versus Amplitude; Part d.): (1, 0) Resonance (f_{1200}) versus Amplitude;
–Lines are from tracking
–Symbols are experimental data

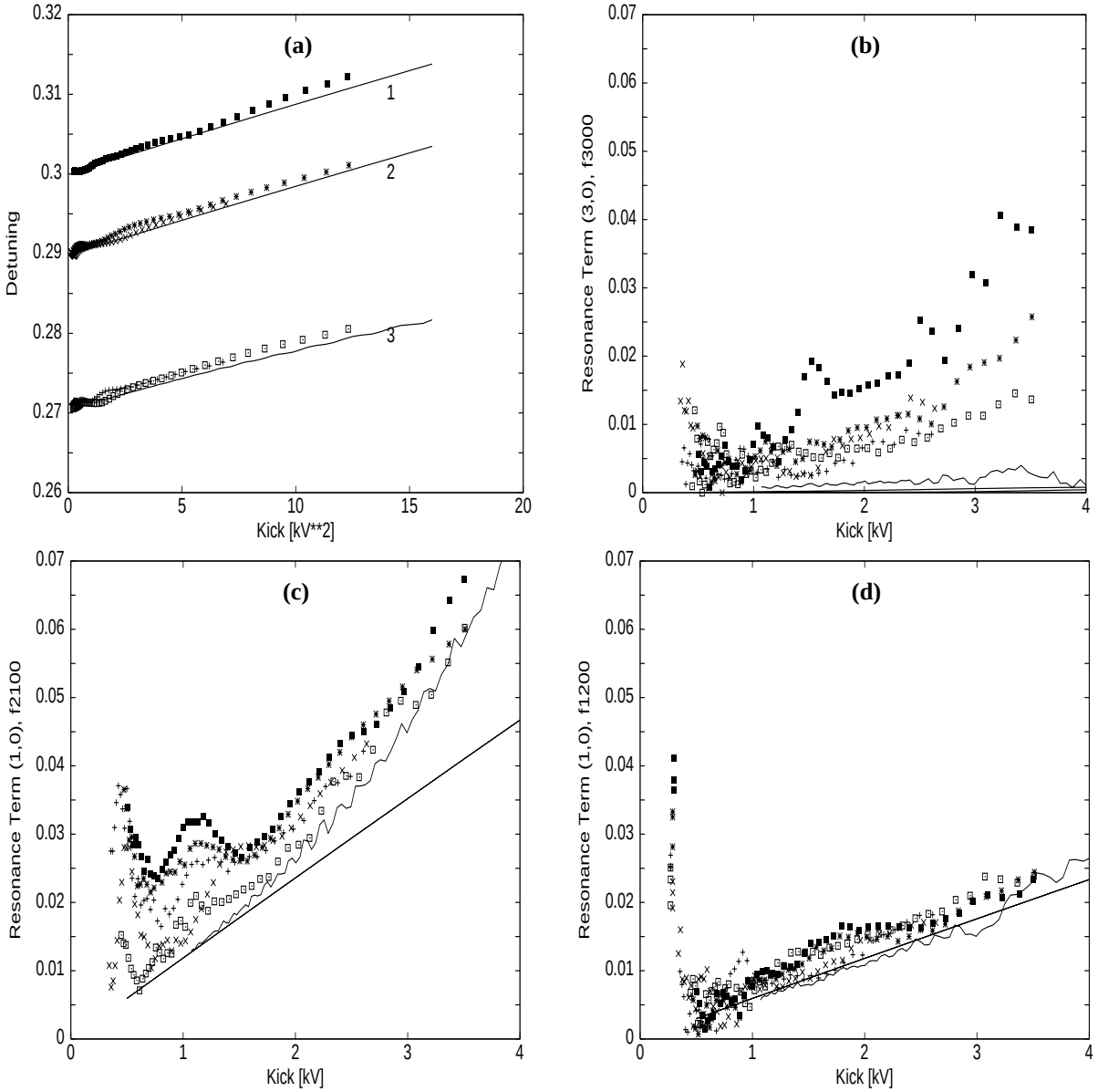

Figure 7: Detuning and First Order Sextupole Driving Terms
Part a.): Detuning versus kick amplitude [kV^2]; Part b.): (3, 0) Resonance versus Amplitude;
Part c.): (1, 0) Resonance (f_{2100}) versus Amplitude; Part d.): (1, 0) Resonance (f_{1200}) versus Amplitude;
–Lines are from tracking
–Symbols are experimental data